TIME-INSTANCE ZERO-CROSSING PRECODING WITH QUALITY-OF-SERVICE CONSTRAINTS

Diana M. V. Melo[1], Lukas T. N. Landau[1], Lucas N. Ribeiro[2], Martin Haardt[2]
[1]Centre for Telecommunications Studies, Pontifical Catholic University of Rio de Janeiro, Rio de Janeiro, Brazil 22453-900
[2]Communications Research Laboratory TU Ilmenau, Ilmenau, Germany
Email: {diana, lukas.landau}@cetuc.puc-rio.br {lucas.ribeiro, martin.haardt}@tu-ilmenau.de

ABSTRACT

Analog-to-digital converters (ADCs) of low-resolution are promising for future wireless communications systems that require low power consumption and low hardware complexity. In this study, we investigate a waveform design for a bandlimited multi-user MIMO downlink scenario with 1-bit quantization and oversampling at the receivers. The novel modulation implies that the information is conveyed into the time instances of zero-crossings. Different to prior studies, the proposed precoding method minimizes the transmit power while taking into account quality of service constraints in terms of the minimum distance to the decision threshold. Unlike the precoding methods with a total power constraint, the bit error rate decreases significantly faster as a function of the average SNR.

Index Terms— 1-bit, quantization, oversampling, precoding, Internet-of-Things

1. INTRODUCTION

Modern communication systems have as requirements the support of a large number of devices and data. One of the most promising applications for future communications is internet of things (IoT). These communications networks require low energy consumption and low complexity devices. In this sense, using a low resolution analog-to-digital converter (ADC) at the receiver could facilitate the realization of simple IoT devices with long battery life.

Achieving resolution in time is less challenging than resolution in amplitude, e.g., [1]. So it is promising to compensate the loss due to 1-bit quantization by oversampling in time w.r.t. the Nyquist rate.

Considering a Zakai bandlimited process, the author in [2] shows that in the noiseless case, rates of $\log_2(M_{\mathrm{Rx}}+1)$ bits per Nyquist interval are achievable by M_{Rx}-fold oversampling. This process is constructed by conveying the information within the time instances of zero-crossings. Studies related to systems with 1-bit quantization and oversampling at the receiver have been conducted for SISO channels as in [3–9]. Moreover, for MIMO systems the studies in [10–12] present novel precoding schemes for 1-bit quantization and oversampling at the receiver. The approaches in [11] and [12] rely on zero-crossing modulation, where unlike the approach in [2], the absence of zero crossing is also considered as a transmit symbol. The study in [11] considers a temporal precoder which maximizes the minimum distance to the decision threshold, while in [12] the temporal and spatial precoder is optimized based on the minimum mean squared error (MMSE) criterion. Moreover, the multiuser MIMO uplink channel with 1-bit quantization and oversampling is studied in [13–15].

In this study, we consider a bandlimited multiuser MIMO downlink system for receivers with 1-bit quantization, considering the novel time instance zero-crossing modulation similar to the approach in [11]. The precoding task is solved based on a convex optimization problem which minimizes the transmit energy per user taking into account the quality of service (QOS) constraint. Similar to the strategy proposed in [16] for intelligent reflecting surfaces, the problem formulation expresses the QOS in terms of the minimum distance to the decision threshold.

The rest of this paper is organized as follows: First, in Sec. 2. the system model is detailed. Afterwards, in Sec. 3 we describe the proposed time-instance zero-crossing modulation, the optimization problem for QOS temporal precoding, and the detection process. Then the numerical results are presented in Sec. 4. Finally, we draw conclusions in Sec. 5.

Notation: In the paper all scalar values, vectors and matrices are represented by a, $\boldsymbol{x}$ and $\boldsymbol{X}$, respectively.

2. SYSTEM MODEL

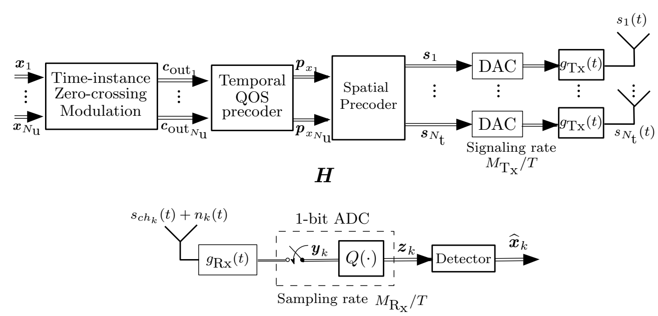

Fig. 1: Multiuser MIMO system model

We consider a multiuser MIMO scenario, as depicted in Fig. 1. The system consists of N_{t} transmitting antennas at the base station (BS) and N_{u} single antenna users. At the BS, the transmit sequence per-user k, denoted as $\boldsymbol{x}_k$, is temporally and spatially precoded.

Initially, each symbol stream $\boldsymbol{x}_k = \boldsymbol{x}_{kI} + j\boldsymbol{x}_{kQ}$, of N complex symbols, is modulated through the *time-instance zero-crossing* (ZC) modulator. The output of the ZC modulator is termed $\boldsymbol{c}_{\mathrm{out}_k} \in \mathbb{C}^{N_{\mathrm{tot}}}$, where $N_{\mathrm{tot}} = M_{\mathrm{Rx}}N+1$ and M_{Rx} is related to the sampling rate $\frac{M_{\mathrm{Rx}}}{T}$. Subsequently, the $\boldsymbol{c}_{\mathrm{out}_k}$ pattern is fed into the temporal QOS precoder which yields the precoded vector $\boldsymbol{p}_{\mathrm{x}_k} \in \mathbb{C}^{N_{\mathrm{q}}}$, where $N_{\mathrm{q}} = M_{\mathrm{Tx}}N+1$ and M_{Tx} is associated to the signaling rate $\frac{M_{\mathrm{Tx}}}{T}$.

Afterwards, the temporally precoded sequences are spatially precoded using the matrix $\boldsymbol{P}_{\mathrm{sp}} \in \mathbb{C}^{N_{\mathrm{t}}\times N_{\mathrm{u}}}$ and converted to a continuous waveform with an ideal digital-to-analog converter (DAC) and the pulse shaping filter with impulse response $g_{\text{Tx}}(t)$. The received signal passes the receive filter with impulse response $g_{\text{Rx}}(t)$ and then is 1-bit quantized. The signal is M_{Rx}-fold oversampled w.r.t the Nyquist rate such that the sampling rate is $\frac{M_{\text{Rx}}}{T} = \frac{M M_{\text{Tx}}}{T}$. The combined waveform determined by the transmit and receive filter is given by $v(t) = g_{\text{Tx}}(t) * g_{\text{Rx}}(t)$.

Furthermore a flat fading channel is considered, described by the channel matrix $\boldsymbol{H} \in \mathbb{C}^{N_{\text{u}} \times N_{\text{t}}}$. The received signal $\boldsymbol{Z} \in \mathbb{C}^{N_{\text{u}} \times N_{\text{tot}}}$ where $N_{\text{tot}} = M_{\text{Rx}}N + 1$ can be expressed by the matrix

$$\boldsymbol{Z} = \text{Q}(\boldsymbol{H}\boldsymbol{P}_{\text{sp}}\boldsymbol{P}_{\text{x}} + \boldsymbol{N}\boldsymbol{G}_{\text{Rx}}^{T}), \tag{1}$$

where $Q(\cdot)$ denotes the element-wise applied quantization operator due to the 1-bit ADC. The matrix $\boldsymbol{P}_{\text{x}}$ is formed by stacking the transmit signal of the N_{u} users, such that

$$\boldsymbol{P}_{\text{x}} = \left[(\boldsymbol{V}\boldsymbol{U}\boldsymbol{p}_{\text{x}_1})^{\text{T}}; (\boldsymbol{V}\boldsymbol{U}\boldsymbol{p}_{\text{x}_2})^{\text{T}}; \ldots; (\boldsymbol{V}\boldsymbol{U}\boldsymbol{p}_{\text{x}_{N_{\text{u}}}})^{\text{T}} \right],$$

where the waveform matrix of dimensions $N_{\text{tot}} \times N_{\text{tot}}$ reads as

$$\boldsymbol{V} = \begin{bmatrix} v(0) & v\left(\frac{T}{M_{\text{Rx}}}\right) & \cdots & v(TN) \\ v\left(-\frac{T}{M_{\text{Rx}}}\right) & v(0) & \cdots & v\left(T\left(N - \frac{1}{M_{\text{Rx}}}\right)\right) \\ \vdots & \vdots & \ddots & \vdots \\ v(-TN) & v\left(T\left(-N + \frac{1}{M_{\text{Rx}}}\right)\right) & \cdots & v(0) \end{bmatrix}. \tag{2}$$

The matrix $\boldsymbol{U}$ which describes the M-fold upsampling operation has dimensions $N_{\text{tot}} \times N_{\text{q}}$ and its entries are defined by

$$\boldsymbol{U}_{m,n} = \begin{cases} 1, & \text{for} \quad m = M \cdot (n-1) + 1 \\ 0, & \text{else.} \end{cases} \tag{3}$$

Moreover, $\boldsymbol{N} \in \mathbb{C}^{N_{\text{u}} \times 3N_{\text{tot}}}$ is the matrix which contains the i.i.d. complex Gaussian noise samples with zero mean and variance σ_n^2. The matrix $\boldsymbol{G}_{\text{Rx}}$ represents the receive filter and reads as

$$\boldsymbol{G}_{\text{Rx}} = a_{\text{Rx}} \begin{bmatrix} \left[\ \boldsymbol{g}_{\text{Rx}}^{T}\ \right] & 0 \cdots & 0 \\ 0 & \left[\ \boldsymbol{g}_{\text{Rx}}^{T}\ \right] & 0 \cdots 0 \\ & \ddots \ddots \ddots & \\ 0 \cdots & 0 & \left[\ \boldsymbol{g}_{\text{Rx}}^{T}\ \right] \end{bmatrix}_{N_{\text{tot}} \times 3N_{\text{tot}}}, \tag{4}$$

with $\boldsymbol{g}_{\text{Rx}} = [g_{\text{Rx}}(-T(N + \frac{1}{M_{\text{Rx}}})), g_{\text{Rx}}(-T(N + \frac{1}{M_{\text{Rx}}}) + \frac{T}{M_{\text{Rx}}}), \ldots, g_{\text{Rx}}(T(N + \frac{1}{M_{\text{Rx}}}))]^{T}$ and $a_{\text{Rx}} = (T/(M_{\text{Rx}}))^{1/2}$ is a normalization factor where we assume a normalized impulse response such that

$$\int_{-\infty}^{\infty} g_{\text{Rx}}(t)^2 dt = 1. \tag{5}$$

Considering perfect channel state information, the conventional spatial zero-forcing (ZF) precoding matrix [17] is described by

$$\boldsymbol{P}_{\text{sp}} = c_{\text{zf}}\boldsymbol{P}_{\text{zf}} \quad \text{with} \quad \boldsymbol{P}_{\text{zf}} = \boldsymbol{H}^{\text{H}}\left(\boldsymbol{H}\boldsymbol{H}^{\text{H}}\right)^{-1}, \tag{6}$$

where the ZF scaling factor is given by

$$c_{\text{zf}} = \left(N_{\text{u}}/\text{trace}\left(\left(\boldsymbol{H}\boldsymbol{H}^{\text{H}}\right)^{-1}\right)\right)^{\frac{1}{2}}. \tag{7}$$

The channel and precoding matrices can be expressed as $\boldsymbol{H}\boldsymbol{P}_{\text{sp}} = \beta\boldsymbol{I}$ where β refers to the beamforming gain. Equation (1) can be rewritten as

$$\boldsymbol{Z} = \text{Q}(\beta\boldsymbol{P}_{\text{x}} + \boldsymbol{N}\boldsymbol{G}_{\text{Rx}}^{T}), \tag{8}$$

Table 1: Time-instance ZC precoding for $M_{\text{Rx}} = 2$.

Input	Output $[\boldsymbol{c}_{\text{s},2i}^{T}, \boldsymbol{c}_{\text{s},2i+1}^{T}]$	
	$p_{2i-1} = +1$	$p_{2i-1} = -1$
000	$+1+1+1+1$	$-1-1-1-1$
001	$+1+1+1-1$	$-1-1-1+1$
011	$+1+1-1-1$	$-1-1+1+1$
010	$+1-1-1-1$	$-1+1+1+1$
110	$+1-1-1+1$	$-1+1+1-1$
111	$-1-1-1+1$	$+1+1+1-1$
101	$-1-1-1-1$	$+1+1+1+1$
100	$-1-1+1+1$	$+1+1-1-1$

Table 2: Time-instance ZC precoding for $M_{\text{Rx}} = 3$.

Input	Output $\boldsymbol{c}_{\text{s},i}^{T}$	
	$p_{i-1} = +1$	$p_{i-1} = -1$
00	$+1+1+1$	$-1-1-1$
01	$+1+1-1$	$-1-1+1$
11	$+1-1-1$	$-1+1+1$
10	$-1-1-1$	$+1+1+1$

and the signal at the k-th user can be written as a column vector as

$$\boldsymbol{z}_k = Q(\beta\boldsymbol{V}\boldsymbol{U}\boldsymbol{p}_{\text{x}_k} + \boldsymbol{G}_{\text{Rx}}\boldsymbol{n}_k), \tag{9}$$

where the vector $\boldsymbol{n}_k \in \mathbb{C}^{3N_{\text{tot}}}$ contains i.i.d. complex Gaussian noise samples with zero mean and variance σ_n^2. The next section describes the temporal precoding method to construct the vector $\boldsymbol{p}_{\text{x}}$ based on a time-instance zero-crossing modulation.

3. PROPOSED TIME-INSTANCE ZERO-CROSSING PRECODING

In this section, the method to construct the precoding vector $\boldsymbol{p}_{\text{x}_k}$ which conveys the information in the zero-crossing time instances of the received signal is described. The process starts with the construction of the desired output pattern $\boldsymbol{c}_{\text{out}_k}$ at the receiver through the time-instance zero-crossing modulator. Then the sequence is feed into the QOS temporal precoding process and finally the spatial precoder is applied.

3.1. Time-Instance Zero-Crossing Mapping

The time-instance zero-crossing modulation has been introduced in the studies [11] and [12]. For channels with 1-bit quantization and oversampling the Nyquist interval can be represented by M_{Rx} samples which implies M_{Rx} sub intervals per symbol.

The symbols with input cardinality $R_{\text{in}} = M_{\text{Rx}} + 1$ are associated to the presence in one of the M_{Rx} sub intervals or the absence of zero-crossing during the Nyquist interval. This means that the information is conveyed into the time-instances of zero-crossings of the signal. With the above method, each symbol can convey $\log_2(M_{\text{Rx}} + 1)$ bits, per real dimension.

In relation to the study proposed in [2] in which the construction of a bandlimited process is presented with zero-crossings in each Nyquist interval, this study considers also the absence of a zero-crossing for one of the symbols from R_{in}, which implies fewer zero-crossings in the entire sequence. The output pattern $\boldsymbol{c}_{\text{out}_k}$ is built in a similar and independent way for all users and for the in-phase and quadrature components of the transmit sequence $\boldsymbol{x}_k$. Each Nyquist interval is mapped into the segment $\boldsymbol{c}_{\text{s},i}$ of M_{Rx} samples, where the information is conveyed within the desired interval. Each $\boldsymbol{c}_{\text{s}}$ segment of each symbol is associated with two different codewords given the dependence on the last sample ρ_{i-1} of the previous segment $\boldsymbol{c}_{\text{s},i-1}$.

Nevertheless, both codewords convey the same information about the allocation of the zero-crossing time-instance. Finally the complete $\boldsymbol{c}_{\text{out}_k}$ pattern of user k is formed by the concatenation of the corresponding $\boldsymbol{c}_{\text{s}}$ segments of each Nyquist interval, which reads as $\boldsymbol{c}_{\text{out}_k} = [p_{\text{b}}, \boldsymbol{c}_{\text{s},0}^T, \ldots, \boldsymbol{c}_{\text{s,N-1}}^T]^T$ of length $NM_{\text{Rx}}+1$. The pilot signal $p_{\text{b}} \in \{1, -1\}$ is included as the first sample due to the dependence of the codeword on the last sample of the previous segment.

The zero-crossing assignments, used in this study, for each symbol are shown in Table 1 and Table 2. In the case of $M_{\text{Rx}} = 2$, three input bits are mapped over two consecutive symbols in order to reduce the conversion loss for this case when mapping bits to symbols. The next section explains the construction of the temporally precoded vector $\boldsymbol{p}_{\text{x}_k}$, given the desired output pattern $\boldsymbol{c}_{\text{out}_k}$.

3.2. Optimization problem for QOS temporal precoding

In the following, we develop a precoding method that minimizes the per user transmit energy E_{0_k} in combination with a constraint on the minimum distance to the decision threshold denoted by γ. This section describes how to obtain the optimal temporal precoding vector $\boldsymbol{p}_{\text{x}_k}$ by solving a convex optimization problem. By considering the spatial ZF precoder, as explained in Sec. 2, the transmit energy per user can be defined by

$$\begin{aligned}\boldsymbol{E}_{0_k} = \boldsymbol{p}_{\text{sp}_k}^{\text{H}} \boldsymbol{p}_{\text{sp}_k} [(\boldsymbol{W}\boldsymbol{p}_{\text{x}_k I})^{\text{T}} (\boldsymbol{W}\boldsymbol{p}_{\text{x}_k I}) + \\ (\boldsymbol{W}\boldsymbol{p}_{\text{x}_k Q})^{\text{T}} (\boldsymbol{W}\boldsymbol{p}_{\text{x}_k Q})],\end{aligned} \tag{10}$$

where $\boldsymbol{p}_{\text{sp}_k}$ denotes the k-th column of $\boldsymbol{P}_{\text{sp}}$, $\boldsymbol{W} = \boldsymbol{G}_{\text{Tx}}^T \boldsymbol{U}$, and $\boldsymbol{G}_{\text{Tx}}$ denotes a Toeplitz matrix of size $N_{\text{tot}} \times 3N_{\text{tot}}$, which is given by

$$\boldsymbol{G}_{\text{Tx}} = a_{\text{Tx}} \begin{bmatrix} [\ \boldsymbol{g}_{\text{Tx}}^T\ ] & 0 \cdots & 0 \\ 0 & [\ \boldsymbol{g}_{\text{Tx}}^T\ ] & 0 \cdots 0 \\ & \ddots \ddots \ddots & \\ 0 \cdots & 0 & [\ \boldsymbol{g}_{\text{Tx}}^T\ ] \end{bmatrix}, \tag{11}$$

with $a_{\text{Tx}} = (T/M_{\text{Tx}})^{1/2}$ and $\boldsymbol{g}_{\text{Tx}} = \left[g_{\text{Tx}}(-T(N+M_{\text{Tx}}^{-1})),\ g_{\text{Tx}}(-T(N+M_{\text{Tx}}^{-1}) + T\,M_{\text{Tx}}^{-1}), \ldots, g_{\text{Tx}}(T(N+M_{\text{Tx}}^{-1}))\right]^T$. The prefactor $\boldsymbol{p}_{\text{sp}_k}^{\text{H}} \boldsymbol{p}_{\text{sp}_k}$ in (10) is independent of $\boldsymbol{p}_{\text{x}_k}$ so it is ignored for the individual optimization problems of the users. The convex optimization problem is solved in a similar and independent way for all users and for the in-phase and quadrature components of the transmit sequence $\boldsymbol{x}_k$. The optimization problem is expressed as a convex quadratic program given by

$$\begin{aligned} \min_{\boldsymbol{p}_{\text{x}_{kI/Q}}} \quad & (\boldsymbol{W}\boldsymbol{p}_{\text{x}_{kI/Q}})^{\text{T}} (\boldsymbol{W}\boldsymbol{p}_{\text{x}_{kI/Q}}) \\ \text{subject to:} \quad & \boldsymbol{B}_k \boldsymbol{p}_{\text{x}_{kI/Q}} \preceq -\gamma \boldsymbol{a}, \end{aligned} \tag{12}$$

where

$$\begin{aligned} \boldsymbol{B}_{\text{k}} &= -\,\beta \left(\boldsymbol{C}_{\text{k}I/Q} \boldsymbol{V}\boldsymbol{U}\right) \\ \boldsymbol{C}_{\text{k}} &= \text{diag}\left(\boldsymbol{c}_{\text{out}_{\text{k}I/Q}}\right) \\ \boldsymbol{a} &= \boldsymbol{1} \in \mathbb{R}^{M_{\text{Rx}}N+1}. \end{aligned} \tag{13}$$

$\boldsymbol{p}_{\text{x}_{kI/Q}}$ represents the in phase or quadrature components of $\boldsymbol{p}_{\text{x}_k}$ this is $\boldsymbol{p}_{\text{x}_{kI}}$ or $\boldsymbol{p}_{\text{x}_{kQ}}$ respectively The constraint in (12) ensures that the noise free received signal after quantization is equal to $\boldsymbol{c}_{\text{out}_{kI/Q}}$. The symbol $\preceq$ in (12) constrains each element of the vector $\boldsymbol{B}_k \boldsymbol{p}_{\text{x}_{kI/Q}}$ to be less than or equal to $-\gamma$ such that the minimum distance of the samples of the received signal to the decision threshold is equal to γ. Implicitly, the optimization problem shapes the waveform $y(t)$ at the receiver, which is described in the discrete model by $\beta \boldsymbol{V}\boldsymbol{U}\boldsymbol{p}_{\text{x}_k}$ for the noiseless case. Considering the matrix $\boldsymbol{P}_{\text{x}_{\text{Tx}}}$ given by

$$\boldsymbol{P}_{\text{x}_{\text{Tx}}} = \left[(\boldsymbol{G}_{\text{Tx}}^{\text{T}} \boldsymbol{U}\boldsymbol{p}_{\text{x}_1})^{\text{T}}; (\boldsymbol{G}_{\text{Tx}}^{\text{T}} \boldsymbol{U}\boldsymbol{p}_{\text{x}_2})^{\text{T}}; \cdots; (\boldsymbol{G}_{\text{Tx}}^{\text{T}} \boldsymbol{U}\boldsymbol{p}_{\text{x}_{N_{\text{u}}}})^{\text{T}}\right]. \tag{14}$$

The total transmit energy per block can be cast as

$$E_{\text{Tx}} = \text{trace}\left(\boldsymbol{P}_{\text{sp}} \boldsymbol{P}_{\text{x}_{\text{Tx}}} \boldsymbol{P}_{\text{x}_{\text{Tx}}}^{\text{H}} \boldsymbol{P}_{\text{sp}}^{\text{H}}\right). \tag{15}$$

The next section describes the detection process at the receiver.

3.3. Detection

The detection process is based on the Hamming distance as considered in prior works [10], [11], and [12]. Given the requirement of low complexity receivers, a simple detection process is favorable. The detection of the time-instance zero-crossing is based on ρ_{i-1} by performing a backward mapping process to the modulation.

Taking into account the received signal (1), sub-sequences $\boldsymbol{z}_{b,i}$ are constructed such that $\boldsymbol{z}_{b,i} = [\rho_{i-1}, \boldsymbol{c}_{\text{s},i-1}] \in \{+1, -1\}^{M_{\text{Rx}}+1}$. Through the sequences $\boldsymbol{z}_b$, it is possible to perform the backward mapping process by detecting the time-instance of the zero-crossing and considering the Tables 1 and 2. The first symbol in the sequence is detected by taking into account the pilot sample p_b.

In a noise free environment it is possible to perform a perfect recovery of the original segment by considering the backward mapping process $\overleftarrow{d}(\cdot)$. However, in the presence of noise the segments $\boldsymbol{z}_b$ may have invalid values. In this case, the detection rules based on the Hamming-distance metric [10] are considered, which read as

$$\widehat{x_i} = \overleftarrow{d}(\boldsymbol{c}), \quad \text{where} \quad \boldsymbol{c} = \arg\min_{\boldsymbol{c}_{\text{map}}} \ \text{Hamming}(\boldsymbol{z}_{b,i}, \boldsymbol{c}_{\text{map}}),$$

where Hamming $(\boldsymbol{z}_{b,i}, \boldsymbol{c}_{\text{map}}) = \sum_{n=1}^{M_{\text{Rx}}+1} \frac{1}{2} |\boldsymbol{z}_{b,i,n} - \boldsymbol{c}_{\text{map},n}|$. The subsequences $\boldsymbol{c}_{\text{map}} = [p_{i-1}, \boldsymbol{c}_{\text{s},i}]^T$ refer to the set of valid codewords presented in Tables 1 and 2.

4. NUMERICAL RESULTS

In this section, the numerical results are presented and discussed. The simulation parameters correspond to $N_{\text{t}} = 8$ transmit antennas and $N_{\text{u}} = 2$ single-antenna users. The number of transmit symbols is $N = 30$. The entries of the channel matrix $\boldsymbol{H}$ are i.i.d. zero-mean complex Gaussian distributed with unit variance. The transmit and receive filters are RC and RRC filters, respectively with $\epsilon_{\text{Rx}} = \epsilon_{\text{Tx}} = 0.22$ as in [10–12]. Furthermore, different values of M_{Rx} and M_{Tx} are considered. Relating γ and the noise power spectral density N_0, we consider that $\gamma = c\,\sigma_{\text{n}}$, where c is a positive scalar value. The signal to noise ratio (SNR) is defined as

$$\text{SNR} = \frac{\overline{E_{\text{Tx}}}/(N_{\text{q}}T)}{N_0(1+\epsilon_{\text{Tx}})/T} = \frac{\overline{E_{\text{Tx}}}}{N_{\text{q}}N_0(1+\epsilon_{\text{Tx}})}, \tag{16}$$

where $\overline{E_{\text{Tx}}}$ is the average transmit energy per block for a given c. Considering the total number of transmit bits N_{b} per user and dimension, the relation E_{b}/N_0 is defined as follows

$$\frac{E_{\text{b}}}{N_0} = \frac{\overline{E_{\text{Tx}}}}{2N_{\text{b}}N_{\text{u}}N_0}, \tag{17}$$

where E_{b} is the average energy per bit. and $N_0 = \sigma_{\text{n}}^2$. In Fig. 2 we compare the average SNR provided by (16) and (15) vs the scalar

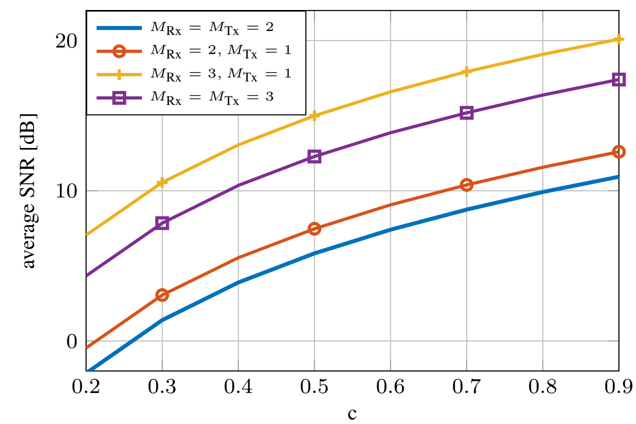

Fig. 2: Average SNR vs QOS constraint

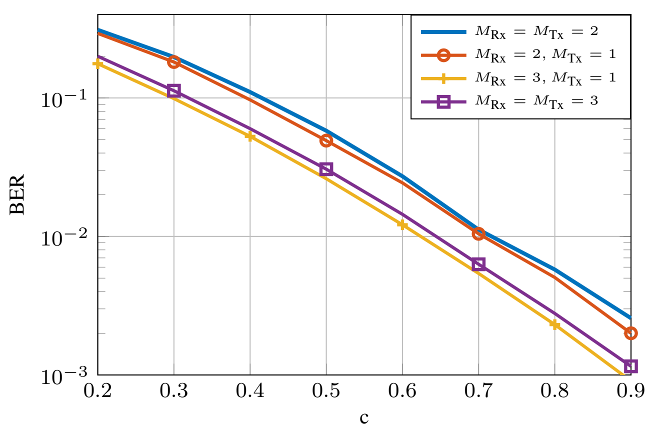

Fig. 3: BER vs QOS constraint

factor c. The simulation results are presented for different sets of M_{Rx} and M_{Tx}. As expected, when increasing the value of c the average SNR increases for all the evaluated configurations. The configuration that achieves higher average SNR values corresponds to $M_{\mathrm{Rx}} = 3, M_{\mathrm{Tx}} = 1$ involving higher transmit energy. The set $M_{\mathrm{Rx}} = M_{\mathrm{Tx}} = 2$ corresponds to the set with the lowest energy requirement for transmission with given QOS. Fig. 3 illustrates the BER against the factor c, which confirms that the considered QOS constraint is a suitable design criterion. Increasing c yields a larger minimum distance to the decision threshold which then improves the detection performance. Fig. 4 we compare the BER vs the average SNR from Fig. 2. As expected the set $M_{\mathrm{Rx}} = 2, M_{\mathrm{Tx}} = 2$ achieves the best performance in terms of the BER. The BER is also presented in terms of the $\frac{E_{\mathrm{b}}}{N_0}$ following (17) as shown in Fig. 5. As expected, the configuration with the best performance is the set $M_{\mathrm{Rx}} = 2, M_{\mathrm{Tx}} = 2$. Note that the case with $M_{\mathrm{Rx}} = 3$ leads to a higher spectral efficiency in comparison to $M_{\mathrm{Rx}} = 2$.

5. CONCLUSIONS

In this work, the zero-crossing precoding method for a bandlimited multi-user MIMO downlink scenario, with 1-bit quantization and oversampling at the receiver, is proposed. Different to prior studies

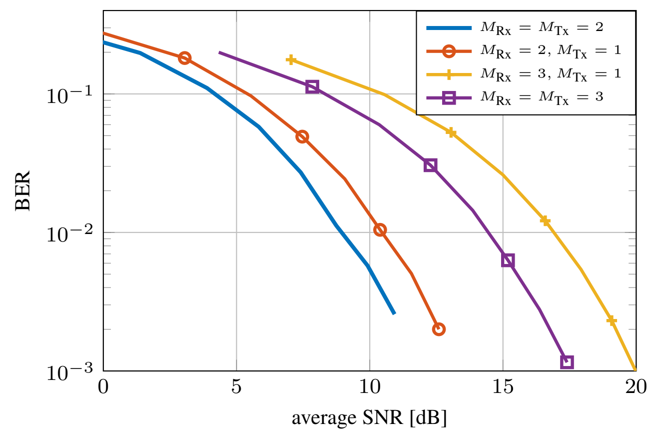

Fig. 4: BER vs average SNR

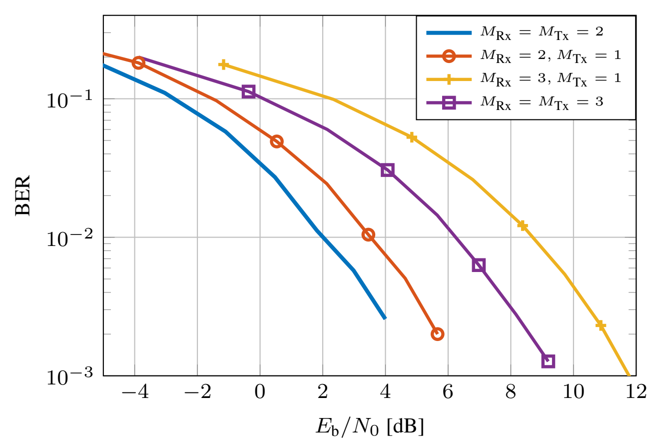

Fig. 5: BER vs E_{b}/N_0

the proposed approach minimizes the transmit energy while taking into account quality of service constraints. The numerical results confirm that the design criterion with QOS constraints is suitable for the realization of reliable communication systems. In contrast to the precoding method with a total power constraint [11], the BER decreases significantly faster with the average SNR.

In the numerical results among the considered scenarios, we found that the minimum transmit energy is achieved for the case $M_{\mathrm{Rx}} = 2, M_{\mathrm{Tx}} = 2$, which corresponds to the best performance in terms of the BER. On the other hand, scenarios with a higher resolution in time with $M_{\mathrm{Rx}} = 3$ support a higher data rate.

6. ACKNOWLEDGMENT

This work has been supported by the ELIOT ANR18-CE40-0030 and FAPESP 2018/12579-7 project.

7. REFERENCES

[1] R.H. Walden, "Analog-to-digital converter survey and analysis," *IEEE J. Sel. Areas Commun.*, vol. 17, no. 4, pp. 539 –550, Apr. 1999.

[2] S. Shamai (Shitz), "Information rates by oversampling the sign of a bandlimited process," *IEEE Trans. Inf. Theory*, vol. 40, no. 4, pp. 1230–1236, July 1994.

[3] L. Landau, S. Krone, and G. P. Fettweis, "Intersymbol-interference design for maximum information rates with 1-bit quantization and oversampling at the receiver," in *Proc. of the Int. ITG Conf. on Systems, Communications and Coding*, Munich, Germany, Jan. 2013.

[4] T. Hälsig, L. Landau, and G. P. Fettweis, "Spectral efficient communications employing 1-bit quantization and oversampling at the receiver," in *Proc. of the IEEE Vehicular Technology Conference (Fall)*, 2014.

[5] H. Son, H. Han, N. Kim, and H. Park, "An efficient detection algorithm for PAM with 1-bit quantization and time-oversampling at the receiver," in *Proc. of the IEEE Vehicular Technology Conference (VTC2019-Fall)*, Honolulu, HI, USA, USA, Sep 2019.

[6] S. Bender, L. Landau, M. Dörpinghaus, and G. P. Fettweis, "Communication with 1-bit quantization and oversampling at the receiver: Spectral constrained waveform optimization," in *Proc. of the IEEE Int. Workshop on Signal Processing Advances in Wireless Communications*, Edinburgh, UK, July 2016.

[7] L. Landau, M. Dörpinghaus, and G. P. Fettweis, "1-bit quantization and oversampling at the receiver: Sequence-based communication," *EURASIP Journal on Wireless Communications and Networking*, 2018.

[8] R. Deng, J. Zhou, and W. Zhang, "Bandlimited communication with one-bit quantization and oversampling: Transceiver design and performance evaluation," vol. 69, no. 2, pp. 845–862, Feb. 2021.

[9] L. Landau, M. Dörpinghaus, and G. P. Fettweis, "1-bit quantization and oversampling at the receiver: Communication over bandlimited channels with noise," *IEEE Commun. Lett.*, vol. 21, no. 5, pp. 1007–1010, 2017.

[10] A. Gokceoglu, E. Björnson, E. G. Larsson, and M. Valkama, "Spatio-temporal waveform design for multiuser massive MIMO downlink with 1-bit receivers," *IEEE J. Sel. Topics Signal Process.*, vol. 11, no. 2, pp. 347–362, March 2017.

[11] D. M. V. Melo, L. T. N. Landau, and R. C. de Lamare, "Zero-crossing precoding with maximum distance to the decision threshold for channels with 1-bit quantization and oversampling," in *ICASSP 2020 - 2020 IEEE International Conference on Acoustics, Speech and Signal Processing (ICASSP)*, Barcelona, Spain, 2020, pp. 5120–5124.

[12] D. M. V. Melo, L. T. N. Landau, and R. C. de Lamare, "Zero-crossing precoding with MMSE criterion for channels with 1-bit quantization and oversampling," in *WSA 2020; 24th International ITG Workshop on Smart Antennas*, Hamburg, Germany, 2020, pp. 1–6.

[13] Z. Shao, L. T. N. Landau, and R. C. de Lamare, "Dynamic oversampling for 1-bit ADCs in large-scale multiple-antenna systems," *IEEE Trans. Commun.*, 2021.

[14] Z. Shao, L. T. N. Landau, and R. C. de Lamare, "Channel Estimation for Large-Scale Multiple-Antenna Systems Using 1-Bit ADCs and Oversampling," *IEEE Access*, vol. 8, pp. 85243–85256, 2020.

[15] Ali Bulut Üçüncü and Ali Özgür Yılmaz, "Oversampling in one-bit quantized massive mimo systems and performance analysis," *IEEE Transactions on Wireless Communications*, vol. 17, no. 12, pp. 7952–7964, 2018.

[16] L. Rang, L. Ming, L. Qian, and A. L. Swindlehurst., "Intelligent reflecting surface based passive information transmission: A symbol-level precoding approach," *arXiv:2007.14738*, 2020.

[17] Q. H. Spencer, A. L. Swindlehurst, and M. Haardt, "Zero-forcing methods for downlink spatial multiplexing in multiuser MIMO channels," *IEEE Trans. Signal Process.*, vol. 52, no. 2, pp. 461–471, Feb 2004.